Thermoelectric properties and crystal structures in Y doped $Ca_3Co_4O_9$

H.Nakatsugawa, H.M.Jeong, and K.Nagasawa
Yokohama National University
79-5 Tokiwadai Hodogaya Yokohama 240-8501 Japan E-mail: naka@ynu.ac.jp

Abstract

We have prepared polycrystalline specimens of Y doped $Ca_3Co_4O_9$ using a conventional solid-state reaction method, and investigated the Y substitution effect on the thermoelectric and magnetic properties. The valence state of Co ions in $[(Ca_{1-x}Y_x)_2CoO_3]_{0.62}CoO_2$ ($0 \leqq x \leqq 0.04$) has been clarified as $Co^{3.2+}$ in CoO_2 sheet and $Co^{3.6+}$ in RS-type BL, respectively. In addition, both a broad minimum at around 100K (T_{SDW}^{on}) and a broad maximum between T_{SS}^{end} and T_{SS}^{on} in the $\rho(T)$ curve correspond to two magnetic transitions, where T_{SS}^{end} and T_{SS}^{on} could correspond to the spin-state transition of Co ions in the CoO_2 sheet and in the RS-type BL, respectively. Furthermore, in x= 0.02 and 0.04 samples, the Seebeck coefficient at 800K show the highest value (S = 176 μ V/K). Therefore, Y doped $Ca_3Co_4O_9$ are potential candidates for the practical use of thermoelectric power generations.

Introduction

Since the discovery of large thermoelectric power in the layered compounds $NaCo_2O_4$ and $Ca_3Co_4O_9$,[1-4] misfit-layered cobalt oxides particularly have attracted much interest as candidates for thermoelectric (TE) materials. The polycrystalline $Ca_3Co_4O_9$ sample typically exhibits S=130 μ V/K, ρ =15m Ω cm and κ =1.0W/mK at room temperature.[4] For practical use, an appreciable decrease in ρ must be achieved because ρ =15m Ω cm at room temperature is about one order of magnitude higher than that of Bi_2Te_3-based TE materials. Figure 1 shows the initial structure model projected in perspective from *b*-axis (left) and from *a*-axis (right). As shown in Fig.1, the crystal structure of $Ca_3Co_4O_9$ consists of an alternate stack of a distorted three-layered rock salt (RS)-type Ca_2CoO_3 block layer (BL) and a CdI_2-type CoO_2 conducting sheet parallel to the *c*-axis.[3,5,6] The CdI_2-type $[CoO_2]$ subsystem and the RS-type $[Ca_2CoO_3]$ BL subsystem have common *a*- and *c*-axes and beta angles. Owing to the size difference between the RS-type BL and the CoO_2 sheet, however, the compound has an incommensurate periodicity parallel to the *b*-axis. The resulting structural formula becomes $[Ca_2CoO_3]_pCoO_2$, where p equals b_{CoO2} / $b_{Ca2CoO3}$ ~ 0.62. Such an incommensurate modulation induces periodic positional displacement of constituent ions. Among the first nearest ionic bonds, Co-O bonds in the RS-type BL have the most significant modulation in this compound. Shimoyama *et al.*[7] have reported that some oxygen sites become deficient in the RS-type BL upon heating by which the chemical formula becomes $[Ca_2CoO_{3-\delta}]_{0.62}CoO_2$, where the oxygen deficiency, δ, changes from 0 to 0.14 and should preferentially occur at sites where the Co-O bonds are highly modulated. Sugiyama *et al.*[8] have presented that $[Ca_2CoO_{3-\delta}]_{0.62}CoO_2$ indicates the existence of two magnetic transitions at around T_{SDW} = 100K and T_{SS} = 400 ~ 600K; the former is a transition from a paramagnetic state to an incommensurate spin-density wave (SDW) state. The latter is a transition of the spin state (SS) of Co ions, i.e., the populations of the low-spin (LS), intermediate-spin (IS), and high-spin (HS) states are most likely to vary gradually with increasing temperature above T_{SS}^{end}=380K. However, detailed study of the temperature dependence of the transition and its effect on the Co valence, which is controlled by the partial substitution for Ca ions and/or the oxygen deficiency, δ have not been reported. Recently, we have studied the modulated crystal structure of divalent Pb ion doped $Ca_3Co_4O_9$ polycrystalline samples.[9] In this study, we have employed a high-resolution powder neutron diffraction technique to investigate the weak modulated crystal structure of trivalent Y ion doped $Ca_3Co_4O_9$ polycrystalline samples. This study was carried out to investigate the valence state of Co ions both in the CoO_2 sheet and in the RS-type BL subsystems.

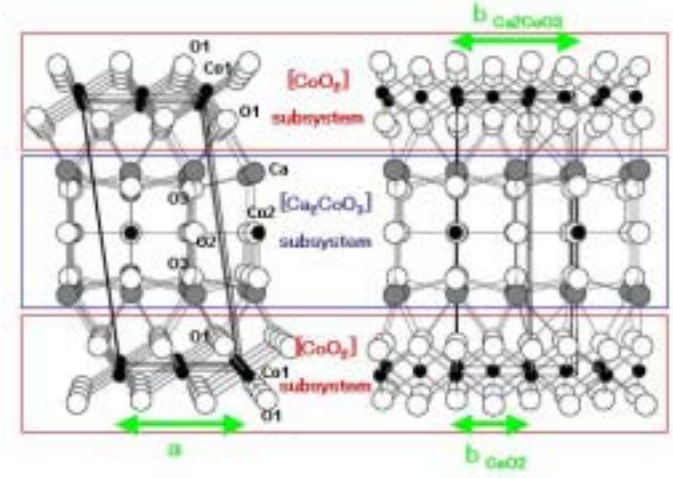

Fig. 1. Initial structure model of $Ca_3Co_4O_9$ projected in perspective from *b*-axis (left) and *a*-axis (right).

Experimental

The polycrystalline samples of $[(Ca_{1-x}Y_x)_2CoO_3]_{0.62}CoO_2$ ($0 \leqq x \leqq 0.04$) were prepared by the conventional solid-state reaction method starting from powder mixture of $CaCO_3$ (99.9 %), Y_2O_3 (99.99%), and Co_3O_4 (99.9 %) with a stoichiometric cation ratio. After calcination in air at 920 ℃ for 12 h, the calcined powders were pressed into pellets at 10MPa. The pellets were sealed into an evacuated vinyl tube and were pressed isostatically at 200MPa. Then the pellets were sintered in flowing pure oxygen gas at 920 ℃ for 24 h. The obtained well-crystallized single-phase samples were annealed in flowing pure oxygen gas at 700 ℃ for 12 h. Bulk density for all samples was about 85% of theoretical density.

The sample homogeneity and crystallinity were confirmed by means of the powder Neutron diffraction (ND) technique. Tne ND data were collected at 293K using the Kinken powder diffractometer for high efficiency and high resolution measurements (HERMES) of Institute for Materials Research (IMR), Tohoku University, installed at the JRR-3M reactor in Japan Atomic Energy Research Institute (JAERI), Tokai.[10] The incident neutron beam was monochromatized at λ =1.8265 Å. The ND data were analyzed using a Rietveld refinement program PREMOS 91 [11] designed for modulated structure analyses. The crystal structures and interatomic distance plots were obtained with the use of PRJMS and MODPLR routines, respectively, both were implemented in the PREMOS 91 package.

Measurements of electrical resistivity and Seebeck coefficient were carried out in temperature range from 80 K to 385 K using Toyo Corporation, ResiTest 8300. The electrical resistivity and the Seebeck coefficient in temperature range from room temperature to 800K were measured using conventional direct current (DC) four-probe method and conventional DC method, respectively. These measurements were carried out in He atmosphere. The magnetic susceptibility was measured using a Quantum Design superconducting quantum interference device (SQUID) magnetic property measurement system (MPMS) under the zero-field cooling (ZFC) and field cooling (FC) conditions in a magnetic field of 10 Oe and in the temperature range from 2K to 350K.

Results and Discussion

Thermoelectric properties

The thermoelectric properties of the polycrystalline specimens of $[(Ca_{1-x}Y_x)_2CoO_3]_{0.62}CoO_2$ ($0 \leqq x \leqq 0.04$) were measured in the temperature range from 80K to 800K. Figure 2 shows the temperature dependence of the electrical resistivity $\rho(T)$ of the samples. All the samples show a broad minimum at around 100K and a broad maximum between 350 K and 600K. It is clearly recognized that the $\rho(T)$ curve shows metallic behavior in the temperature range from T_{SDW}^{on} = 100K to room temperature and an abrupt change in the temperature range from T_{SS}^{end} = 380K to T_{SS}^{on} = 600K, where T_{SS}^{end} and T_{SS}^{on} could correspond to the spin-state transition of Co ions in the CoO_2 sheet and in the RS-type BL, respectively.[8] With a further decrease in temperature below T_{SDW}^{on}, the $\rho(T)$ curve shows a semiconducting behavior owing to the carrier localization of a ferromagnetic transition at around 20K. Sugiyama *et al*.[8] have suggested that a short range incommensurate (IC) SDW order appears below 100K (T_{SDW}^{on}) and the spin-state of Co ions changes above 380K (T_{SS}^{end}).Below 380K, the spin-state of Co ions are LS state. These two magnetic transitions correspond to both a broad minimum at around 100K (T_{SDW}^{on}) and a broad maximum between T_{SS}^{end} and T_{SS}^{on} in the $\rho(T)$ curve. Table 1 shows the electrical resistivity together with the Seebeck coefficient at 800K of all samples. As is clear seen, only the x=0.03 sample exhibits large electrical resistivity. Above T_{SS}^{on}, ρ remains almost constant at about 10 mΩcm except the x=0.03 sample.

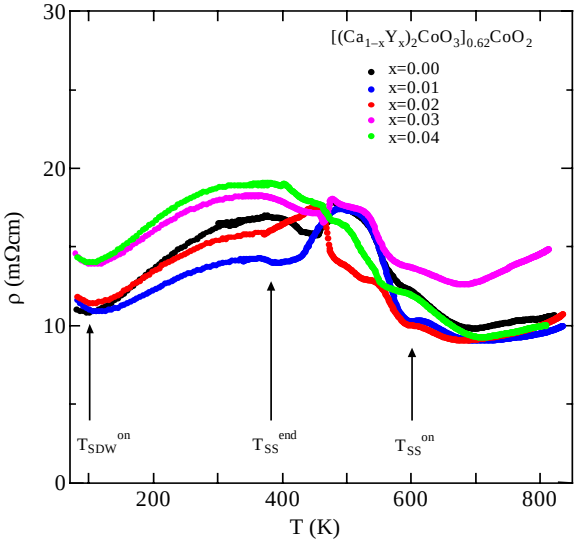

Fig. 2. Temperature dependence of electrical resistivity ρ of . $[(Ca_{1-x}Y_x)_2CoO_3]_{0.62}CoO_2$ ($0 \leqq x \leqq 0.04$).

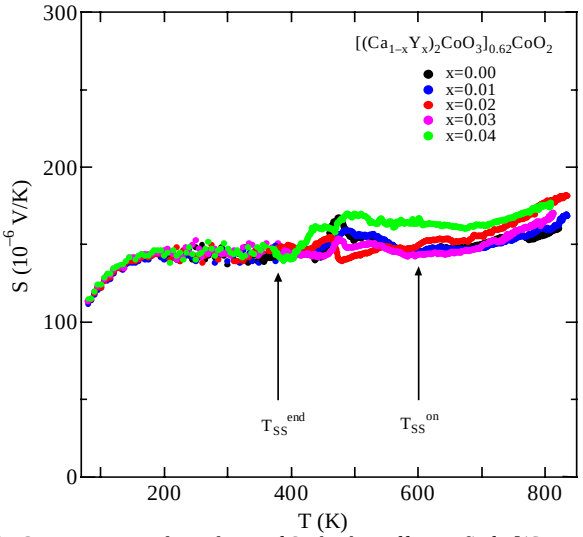

Fig. 3. Temperature dependence of Seebeck coefficient S of . $[(Ca_{1-x}Y_x)_2CoO_3]_{0.62}CoO_2$ ($0 \leqq x \leqq 0.04$).

Table 1. Electrical resistivity ρ, Seebeck coefficient S, power factor S^2/ρ, and dimensionless figure of merit ZT at 800K.Thermal conductivity κ at room temperature,[4] where κ can be expressed by the sum of the lattice component κ_L and the electronic component κ_e, which is estimated from Wiedemann- Franz's law as $\kappa_e = LT/\rho$, where $L = 2.44 \times 10^{-8}$ V^2/K^2 is the Lorentz number. In particular, ZT@800K is estimated using thermal conductivity κ at room temperature[4] for all samples.

	x = 0	x = 0.01	x = 0.02	x = 0.03	x = 0.04
ρ@800K (10^{-3} Ωcm)	10.4	9.4	9.8	14.4	9.8
S@800K (10^{-6} V/K)	156	160	176	166	176
S^2/ρ@800K (10^{-4} W/mK^2)	2.34	2.72	3.16	1.91	3.16
κ @ 300K (W/mK)	0.98	—	—	—	—
ZT@800K	0.19	0.22	0.26	0.16	0.26

Figure 3 shows the temperature dependence of the Seebeck coefficient $S(T)$ of the samples in the temperature range from 80K to 800K. It can be observed clearly that the Seebeck coefficient shows a weak temperature dependence in the temperature range from 100K (T_{SDW}^{on}) to 380K (T_{SS}^{end}). On the other hand, the Seebeck coefficient shows an abrupt change in the spin-state transition temperature between T_{SS}^{end} and T_{SS}^{on}. Abobe T_{SS}^{on} the $S(T)$ curve of all the samples increase monotonically with increasing temperature. Table 1 shows the Seebeck coefficient at 800K of all samples. As is clear seen, the x= 0.02 and 0.04 samples show the highest value, i.e., S@800K=176 μ V/K. Thus, the power factor S^2/ρ and the dimensionless figure of merit ZT at 800K are the highest value, i.e., 3.16×10^{-4} W/mK^2 and 0.26, respectively.

Crystal structure refinement

First, we assumed the superspace group of *C2/m(0 p 0)s0* for the crystal structure of $[(Ca_{0.98}Y_{0.02})_2CoO_3]_{0.62}CoO_2$ (x = 0.02), and assigned the CoO_2 sheet for subsystem 1 and the RS-type BL for subsystem2. In this superspace group, the CoO_2 sheet has *C2/m* symmetry while the RS-type BL subsystem has $C2_1/m$ symmetry and they have an incommensurate period, $p \sim 0.62$, parallel to the *b*-axis.The translation parts of the (3+1)-dimensional symmetry can be written as (0,0,0,0; 1/2,1/2,0,1/2) and the symmetry operations are expressed as x_1, x_2, x_3, x_4; $x_1, -x_2, x_3, -x_4$; $-x_1, x_2, -x_3, x_4+1/2$; $-x_1, -x_2, -x_3, -x_4+1/2$. Table 2 shows a summary of the corresponding fractional coordinates of the atoms in $[(Ca_{0.98}Y_{0.02})_2CoO_3]_{0.62}CoO_2$ (x = 0.02). In the refinement procedure, the thermal displacement parameter B of each atom was assumed to be isotropic.

After two or three refinement cycles, the modulation of the atomic positions in x=0.02 was introduced, considering up to the second order of cosine and sine components of the Fourier terms, i.e., A_i (i = 0, 1, 2) and B_i (i = 1, 2). Table 3 shows a summary of the refined Fourier amplitudes of the positional parameters. Figure 4 shows the observed, calculated and difference intensities of the HERMES data for x = 0.02. Short vertical lines below the patterns indicate the peak positions of the main (upper) and satellite (lower) reflections for the CoO_2 sheet and RS-type BL subsystems. The difference between the observed and calculated patterns is shown below the vertical lines. The final R_{wp} factor is 5.91 % and the lattice parameters are refined to a = 4.8300(5) Å, b_1 = 2.8220(1) Å for CoO_2 sheet, b_2 = 4.5517(1) Å for RS-type BL subsystem, c = 10.838(9) Å and β = 98.130(8) °.

Table 2. Initial structure model for $[(Ca_{0.98}Y_{0.02})_2CoO_3]_{0.62}CoO_2$ (x=0.02).

[CoO2] sheet	x (= x_1)	y (= x_2)	z (= x_3)	B (Å^2)
Co1	0	0	0	1.0
O1	0.359	0	0.0941	1.0
RS-type BL subsystem	x (= x_1)	y (= x_4)	z (= x_3)	B (Å^2)
Ca	0.3207	0	0.7232	1.0
Co2	3/4	0	1/2	1.0
O2	1/4	0	1/2	1.0
O3	0.6970	0	0.3351	1.0

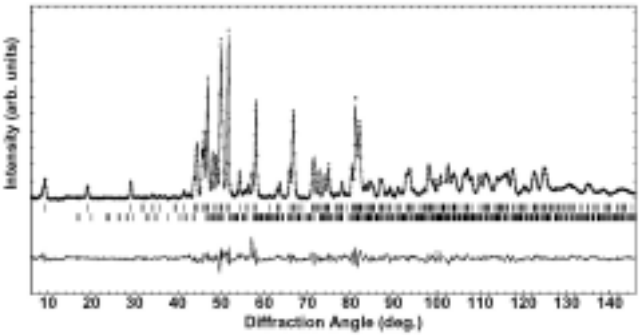

Fig.4 Observed, calculated and difference intensities of ND data for $[(Ca_{0.98}Y_{0.02})_2CoO_3]_{0.62}CoO_2$ (x=0.02).

Table 3. Refined Fourier amplitudes of fractional coordinates and thermal parameters, B, for $[(Ca_{0.98}Y_{0.02})_2CoO_3]_{0.62}CoO_2$ (x=0.02).

[CoO2] sheet		A_0	A_1	B_1	A_2	B_2
Co1	x	0	0.006(0)	0	0	0
	y	0	0	0	0	0
	z	0	0	0	0	0
	B	−0.5(0)				
O1	x	0	−0.009(4)	0	0.003(7)	0
	y	0	0	0.009(4)	0	0.003(8)
	z	0	−0.004(3)	0	0	0
	B	−0.4(5)				
RS-type BL subsystem		A_0	A_1	B_1	A_2	B_2
Ca	x	0	−0.017(8)	0	0.030(8)	0
	y	0	0	−0.008(0)	0	0
	z	0	0	0	0.016(5)	0
	B	−0.2(0)				
Co2	x	0	0.080(0)	0	0	0
	y	0	0	0	0	0.056(3)
	z	0	−0.011(4)	0	0	0
	B	1.6(1)				
O2	x	0	0.116(0)	0	0	0
	y	0	0	0	0	0.066(7)
	z	0	0	0	0	0
	B	0.8(6)				
O3	x	0	−0.008(3)	0	0.011(9)	0
	y	0	0	0.023(0)	0	−0.024(4)
	z	0	0.002(5)	0	−0.015(5)	0
	B	−0.9(6)				

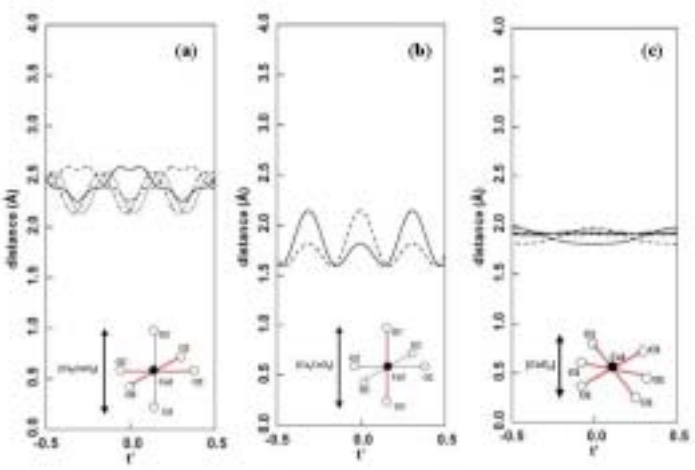

Fig.5 Modulation of (a) four Co2-O2 distances, (b) two Co2-O3 distances, and (c) six Co1-O1 distances against complementary coordinate $t' \sim -0.62x_2 + x_4$ in superspace for $[(Ca_{0.98}Y_{0.02})_2CoO_3]_{0.62}CoO_2$ (x=0.02).

Magnetic susceptibilities

Let us evaluate the valence state of Co ions in $[(Ca_{0.98}Y_{0.02})_2CoO_3]_{0.62}CoO_2$ (x = 0.02). Figure 6 shows the temperature dependence of the inverse-magnetic susceptibility $1/(\chi - \chi_0)$ for x = 0.02 measured under the ZFC condition at a magnetic field of 10 Oe. As shown in Fig. 6, x = 0.02 sample exhibits a positive curvature characteristic of the ferrimagnetic compound. On the basis of mean-field-approximation theory,[12] the magnetic susceptibility can be expressed as

$$\chi = \chi_0 + \frac{(C_{Co1} + C_{Co2})T - 2T_C\sqrt{C_{Co1} \cdot C_{Co2}}}{T^2 - T_C{}^2},$$

where χ_0 is the temperature-independent term and C_{co1} and C_{co2} are the Curie constants of Co ions contributed by the $[CoO_2]$ and $[Ca_2CoO_3]$ subsystems, respectively. By appropriately fitting the $1/(\chi - \chi_0)$ data above 30 K, for example, we obtained C_{co1}=0.062 and C_{co2}=0.213 emu K/mol(Co) for x = 0.02. Using these parameters, the average valence state of Co ions was determined to be $Co1^{3.22+}$ and $Co2^{3.64+}$ for x = 0.02. The resulting nominal valence state of Co ions, i.e., $(3.22+3.64\times0.62)/1.62=3.38$, shows a good agreement with the calculated value on the basis of the charge neutrality of the chemical formula $Ca_{1.22}Y_{0.02}Co^{3.38+}{}_{1.62}O_{3.99}$, i.e., $[(Ca_{0.98}Y_{0.02})_2CoO_{3.21}]_{0.62}CoO_2$.

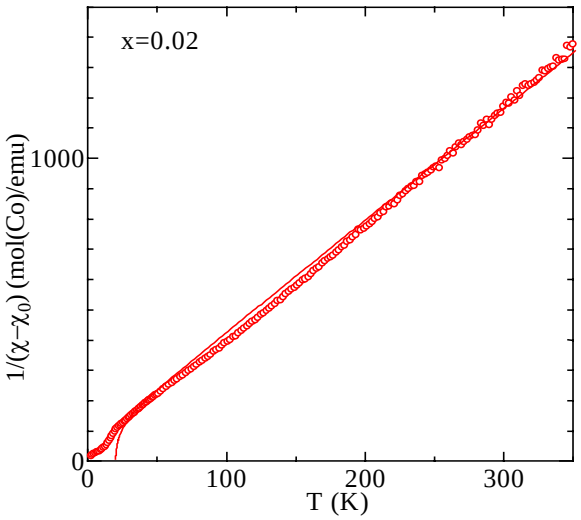

Fig.6 Temperature dependence of inverse magnetic susceptibility $1/(\chi - \chi_0)$ for $[(Ca_{0.98}Y_{0.02})_2CoO_3]_{0.62}CoO_2$ (x = 0.02), where solid line shows result of appropriately fitting $1/(\chi - \chi_0)$ plots, where $\chi_0 \sim 8.4\times10^{-4}$ emu/mol(Co) is temperature independent term and T_C=19K is ferromagnetic transition temperature.

Conclusions

The valence state of Co ions in $[(Ca_{1-x}Y_x)_2CoO_3]_{0.62}CoO_2$ ($0 \leqq x \leqq 0.04$) has been clarified as $Co^{3.2+}$ in CoO_2 sheet and $Co^{3.6+}$ in RS-type BL, respectively. In addition, both a broad minimum at around 100K ($T_{SDW}{}^{on}$) and a broad maximum between $T_{SS}{}^{end}$ and $T_{SS}{}^{on}$ in the $\rho(T)$ curve correspond to two magnetic transitions, where $T_{SS}{}^{end}$ and $T_{SS}{}^{on}$ could correspond to the spin-state transition of Co ions in the CoO_2 sheet and in the RS-type BL, respectively. Furthermore, in x= 0.02 and 0.04 samples, the Seebeck coefficient at 800K show the highest value (S = 176 μ V/K). Therefore, Y-doping is an effective method to improve the thermoelectric performance of $Ca_3Co_4O_9$

Acknowledgments

The authors thank Dr. Y.Okamoto for technical advice in the cold isostatic press and the measurement of high temperature. The Hall effect measurement system (Toyo Corporation, ResiTest 8300) in the Instrumental Analysis Center and the SQUID magnetometer (Quantum Design, MPMS) in the Ecotechnology System Laboratory, Yokohama National University, were used. This study was partly supported by the IWATANI NAOJI foundation and the IKETANI foundation for promotion of science and engineering.

References

1. Terasaki, I. *et al*, "Large thermoelectric power in $NaCo_2O_4$ single crystals," *Phys. Rev. B*, Vol.56, (1997), pp.R12685-R12687.
2. Li, S. *et al*, "High temperature thermoelectric properties of oxide $Ca_9Co_{12}O_{28}$," J. *Mater. Chem*., Vol.9, (1999), pp.1659-1660.
3. Masset, A. C. *et al*, "Misfit-layered cobaltite with an anisotropic giant magnetoresistance: $Ca_3Co_4O_9$," *Phys. Rev. B*, Vol.62, (2000), pp.166-175.
4. Miyazaki, Y. *et al*, "Low-Temperature Thermoelectric Properties of the Composite Crystal $[Ca_2CoO_{3.34}]_{0.614}[CoO_2]$," *Jpn. J. Appl. Phys*., Vol.39, (2000), pp.L531-L533.
5. Lambert S. *et al*, "Three Forms of the Misfit Layered Cobaltite $[Ca_2CoO_3]$ $[CoO_2]_{1.62}$ A 4D Structural Investigation," *J. Solid State Chem*., Vol.160, (2001), pp.322-331.
6. Miyazaki Y. *et al*, "Modulated Structure of the Thermoelectric Compound $[Ca_2CoO_3]_{0.62}CoO_2$," *J. Phys. Soc. Jpn.*, Vol.71, (2002), pp.491-497.
7. Shimoyama J. *et al*, "Oxygen Nonstoichiometry in Layered Cobaltite $Ca_3Co_4O_y$," *Jpn. J. Appl. Phys*., Vol.42, No.2B (2003), pp.L194-L197.
8. Sugiyama J. *et al*, "Hidden magnetic transitions in the thermoelectric layered cobaltite [Ca2CoO3]0.62[CoO2]," *Phys.Rev.* B, Vol.68, (2003), pp.134423.
9. Nakatsugawa H. *et al*, "Thermoelectric and Magnetic Properties of $[(Ca_{1-x}Pb_x)_2CoO_{3.1}]_{0.62}CoO_2$ ($0<x<0.03$)," *Jpn.J.Appl.Phys.*, Vol.46, No.5A (2007), pp.3004-3012.
10. Ohoyama K. *et al*, "The New Neutron Powder Diffractometer with a Multi-Detector System for High-Efficiency and High-Resolution Measurements,",*Jpn. J. Appl. Phys*., Vol.37, No.6A (1998), pp.3319-3326.
11. Yamamoto A., "Determination of composite crystal structures and superspace groups," *Acta Cryst. A*, Vol.49, (1993), pp.831-846.
12. C. Kittel, Introduction to Solid State Physics John Wiley & Sons, (New York, 1996, 7th ed.), pp.461.